The EMBO Journal (2008) 27, 1073–1084 | © 2008 European Molecular Biology Organization | All Rights Reserved 0261-4189/08
www.embojournal.org

THE EMBO JOURNAL

Proteolysis of AKAP121 regulates mitochondrial activity during cellular hypoxia and brain ischaemia

Annalisa Carlucci[1], Annagrazia Adornetto[2], Antonella Scorziello[2], Davide Viggiano[2], Mariapaola Foca[1], Ornella Cuomo[2], Lucio Annunziato[2], Max Gottesman[3] and Antonio Feliciello*[,1]

[1]Dipartimento di Biologia e Patologia Cellulare e Molecolare, Università ''Federico II'', Naples, Italy; [2]Divisione di Farmacologia, Dipartimento di Neuroscienze, Università ''Federico II'', Naples, Italy and [3]Institute of Cancer Research, Columbia University, New York, NY, USA

A-kinase anchor protein 121 (AKAP121) assembles a multivalent signalling complex on the outer mitochondrial membrane that controls persistence and amplitude of cAMP and src signalling to mitochondria, and plays an essential role in oxidative metabolism and cell survival. Here, we show that AKAP121 levels are regulated post-translationally by the ubiquitin/proteasome pathway. Seven In-Absentia Homolog 2 (Siah2), an E3–ubiquitin ligase whose expression is induced in hypoxic conditions, formed a complex and degraded AKAP121. In addition, we show that overexpression of Siah2 or oxygen and glucose deprivation (OGD) promotes Siah2-mediated ubiquitination and proteolysis of AKAP121. Upregulation of Siah2, by modulation of the cellular levels of AKAP121, significantly affects mitochondrial activity assessed as mitochondrial membrane potential and oxidative capacity. Also during cerebral ischaemia, AKAP121 is degraded in a Siah2-dependent manner. These findings reveal a novel mechanism of attenuation of cAMP/PKA signaling, which occurs at the distal sites of signal generation mediated by proteolysis of an AKAP scaffold protein. By regulating the stability of AKAP121-signalling complex at mitochondria, cells efficiently and rapidly adapt oxidative metabolism to fluctuations in oxygen availability.

The EMBO Journal (2008) **27,** 1073–1084. doi:10.1038/emboj.2008.33; Published online 6 March 2008
Subject Categories: proteins; signal transduction
Keywords: AKAP; hypoxia; mitochondria; Siah2; ubiquitin

Introduction

G-protein-dependent activation of adenylate cyclase by extracellular stimuli induces transient increases in intracellular cAMP levels. cAMP binding to its intracellular receptors affects many biological processes, including cell metabolism, growth, differentiation and survival; activity of ion channels and receptors; motility, hormone synthesis and secretion; synaptic transmission; learning and memory (Taylor *et al*, 2005). Protein kinase A (PKA) is a major effector of cAMP. Binding of cAMP to the regulatory subunit of PKA dissociates the holoenzyme. The catalytic subunit then phosphorylates and modulates the activity of several intracellular substrates. PKA signal transduction is controlled by families of specific anchor proteins (A-kinase anchor proteins, AKAPs) that bind and target PKA to distinct subcellular compartments. AKAPs recruit PKA holoenzyme close to its substrate/effector proteins, directing and amplifying the biological effects of cAMP signaling. In addition to PKA, AKAPs complex with additional signalling molecules, including other serine/threonine kinases tyrosine phosphatases, cAMP-phospshodiesterases and membrane adenylyl cyclase. The macromolecular signalling complex nucleated by AKAP constitutes a 'transduceosome', a biological relay that integrates and controls the rate, magnitude and persistence of signals derived from distinct transduction pathways (Feliciello *et al*, 1997, 2001; Tasken and Aandahl, 2004; Wong and Scott, 2004; Barman *et al*, 2006; Dell'Acqua *et al* 2006; Newhall *et al*, 2006).

Mitochondrial AKAPs (AKAP84, AKAP100, AKAP121 and the human homologue AKAP149, also named D-AKAP1) belong to a distinct family of proteins that bind and target PKA to the outer membrane of mitochondria. These proteins are splice variants of the same gene (AKAP1) that share the same N-terminus (residues 1–525), but differ at the C-terminus. The mitochondrial targeting domain is positioned within the first 30 N-terminal residues, whereas the PKA-binding domain resides in the middle segment of the molecule (residues 306–325) (Chen *et al*, 1997; Huang *et al*, 1997). AKAP121 and AKAP149 contain a conserved sequence, the KH domain, which binds the 3′-untranslated regions of nuclear mRNAs that encode mitochondrial proteins F_{o-f} subunit of ATP synthase and MnSOD (Ginsberg *et al*, 2003). Localization of PKA in proximity to mitochondrial substrates ensures efficient propagation of cAMP signals from cell membrane to this target organelle (Harada *et al*, 1999; Affaitati *et al*, 2003; Pagliarini and Dixon, 2006).

Expression of some AKAPs, including AKAP121, is induced at the transcriptional level by hormones that activate adenylyl cyclase (Feliciello *et al*, 1998; Hunzicker-Dunn *et al*, 1998). Accumulation of AKAP121 under the control of cAMP/PKA pathway represents a positive feedback loop between membrane-generated signals and downstream effectors of cAMP. AKAP121/84 interact with PTPD1, a non-receptor tyrosine phosphatase that binds to and activates src tyrosine kinase (Cardone *et al*, 2004). Targeting of PTPD1/src complex to mitochondria enhances cytochrome *c* oxidase

*Corresponding author. Dipartimento di Biologia e Patologia Cellulare e Molecolare, Università Federico II, via S Pansini, 5, Naples 80131, Italy. Tel.: +39 081 7463 615; Fax: +39 081 7463 252;
E-mail: feliciel@unina.it

Received: 5 September 2007; accepted: 8 February 2008; published online: 6 March 2008

activity, mitochondrial membrane potential ($\Delta\Psi_m$) and ATP oxidative synthesis (Livigni *et al*, 2006).

This work describes for the first time a mechanism where signal attenuation at the distal organelles is governed by turnover of an AKAP scaffold protein. We show that hypoxic conditions promote rapid degradation of AKAP121 through the ubiquitin (Ub)–proteasome pathway in both cell culture and rat brain. The responsible Ub ligase is Seven In-Absentia Homolog 2 (Siah2), a hypoxia-induced protein that binds and ubiquitinates AKAP121. The resultant decrease in AKAP121 significantly reduces mitochondrial activity.

Results

Siah2 binds to, and promotes proteasomal degradation of, AKAP121

A cDNA library derived from monocyte/macrophage mRNAs inserted into the yeast vector pGAD–Not was screened using as bait a cDNA encoding AKAP121 residues 329–573 in the yeast plasmid, pGBD10 (pGBD–$A121_{329-573}$) (Figure 1A). One clone (AKAPBP-M) isolated by this selection carried an open reading frame encoding a 214-amino-acid polypeptide corresponding to residues 112–325 of mouse seven-in-absentia protein (Siah2) (Figure 1B). The Siah family are Really Interesting New Gene (RING) proteins that function as Ub ligases and promote degradation of multiple cellular targets (Hu *et al*, 1997; Li *et al*, 1997; Tang *et al*, 1997; Boehm *et al*, 2001; Frew *et al*, 2003; Oliver *et al*, 2004; Gutierrez *et al*, 2006) Co-transfection of pGBD–$A121_{329-573}$ and pGAD–AKAPBP-M strongly activated transcription of *his* and *lacZ* reporter genes in yeast strain YRG2 (data not shown).

To measure *in vitro* association between AKAP121 and Siah2, we engineered an AKAP fusion carrying the N-terminus of AKAP121 appended to the C-terminus of maltose-binding protein (MBP). The fusion protein (MBP–AKAP121) was expressed in *Escherichia coli*, affinity-purified on an amylose column and subjected to pull-down experiments with purified glutathione-*S*-transferase (GST)–Siah2. Figure 1C shows that MBP–AKAP121 efficiently bound recombinant Siah2. In a second experiment, *in vitro* translated, ^{35}S-labeled AKAP121 and haemagglutinin (HA)-tagged Siah2 immunoprecipitated with anti-HA antibody or control IgG. Precipitates were resolved on sodium dodecyl sulphate–polyacrylamide gel electrophoresis (SDS–PAGE) and the recovered proteins were visualized by autoradiography. Figure 1D confirms binding of AKAP121 to Siah2. Next, we determined whether AKAP121 could bind to Siah2 *in vivo*. As Siah2 induces proteasomal degradation of AKAP121 (see below), human embryonic kidney 293 (HEK293) cells were transiently co-transfected with AKAP121 and a Flag-tagged Siah2 ring mutant, which lacks E3–Ub ligase activity ($Siah2_{rm}$), but still binds its substrates (Nakayama *et al*, 2004).

Cell lysates were subjected to co-immunoprecipitation using anti-Flag and anti-AKAP121 antibodies. Figure 1E shows that Siah2 forms a stable complex with AKAP121 and with its endogenous human homologue AKAP149. To determine whether AKAP121 targets Siah2 on mitochondria in intact cells, we performed co-fractionation experiments. Mitochondrial and supernatant fractions were isolated from cells co-transfected with AKAP121 and $Siah2_{rm}$, and immunoblotted with the indicated antibodies. Figure 1F shows that AKAP121 and AKAP149 co-purified with the mitochondria-enriched fraction, as did the voltage-dependent anion channel (VDAC), a protein residing on the outer mitochondrial membrane, whereas β-tubulin was found exclusively in the supernatants. As predicted, in control cells most of $Siah2_{rm}$ protein was found in the supernatant. Expression of AKAP121 significantly increased the amount of $Siah2_{rm}$ recovered in the mitochondrial fraction.

Localization of Siah2 on mitochondria was also demonstrated by immunostaining. Mouse fibroblasts express endogenous AKAP121 that colocalizes exclusively on mitochondria (Cardone *et al*, 2004). Fibroblasts were transfected with HA-tagged Siah2 and immunostained with anti-AKAP121 and anti-HA antibodies. The signals were collected and analysed by confocal microscopy. Figure 1G shows that AKAP121 and HA staining partly overlapped, suggesting that both proteins can colocalize on mitochondria *in vivo*.

To determine whether Siah2 destabilized AKAP121, HEK293 cells were transiently transfected with the expression vectors for AKAP121 and HA-tagged Siah2. Twenty-four hours post-transfection, cells were harvested, lysed and immunoblotted with anti-HA and anti-AKAP121 antibodies. Figure 2A shows that co-transfection with Siah2 almost completely eliminated the accumulation of AKAP121 and decreased AKAP149 (endogenous splice variant). To demonstrate that loss of AKAP121 was mediated by proteasome-dependent degradation, HEK293 cells transfected with AKAP121 and Siah2 were exposed to the proteasome inhibitor, MG132. As shown in Figures 2B and C, MG132 partially reversed the loss of AKAP121 induced by Siah2. The Siah2 ring motif is required for AKAP121 degradation. Thus, transfection with $Siah2_{rm}$ did not reduce AKAP121 levels (Figure 2D). Binding to Siah2 was required for AKAP121 degradation. $AKAP121_{\Delta 336-550}$, a mutant lacking the Siah2-binding domain, was resistant to coexpressed Siah2 (Figure 2E).

Oxygen and glucose deprivation promotes degradation of AKAP121

Transcription of Siah2 is induced by oxygen deprivation (Nakayama *et al*, 2004). Siah2 accumulates during hypoxia and promotes degradation of prolyl-hydroxylases 1 and 3 (PHD1/3). Under physiological conditions, PHDs are required for proteasomal degradation of hypoxia inducible factor (HIF), a transcriptional regulator of hypoxia-induced genes. We asked whether hypoxic conditions also promoted degradation of AKAP121. For the hypoxia experiments, we performed oxygen and glucose deprivation (OGD), an *in vitro* cellular model mimicking the hypoxic conditions occurring *in vivo* during ischaemia (Chavez *et al*, 2006; Liu *et al*, 2006).

HEK293 cells were transiently transfected with either cytomegalovirus (CMV) or AKAP121 vectors. Twenty-four post-transfection, cells were oxygen/glucose deprived for 2 or 4 h. Cell lysates were immunoblotted with anti-HA and anti-AKAP121 antibodies. Figures 3A and B show time-dependent disappearance of AKAP121 and AKAP149 during OGD. Similarly, oxygen deprivation alone (hypoxia) was sufficient to promote AKAP121 degradation (Supplementary Figure S1).

To document the role of endogenous Siah2 in OGD-induced degradation of AKAP121, the $Siah2_{rm}$ vector was added to the AKAP121 transfection mixture. Strikingly, $Siah2_{rm}$

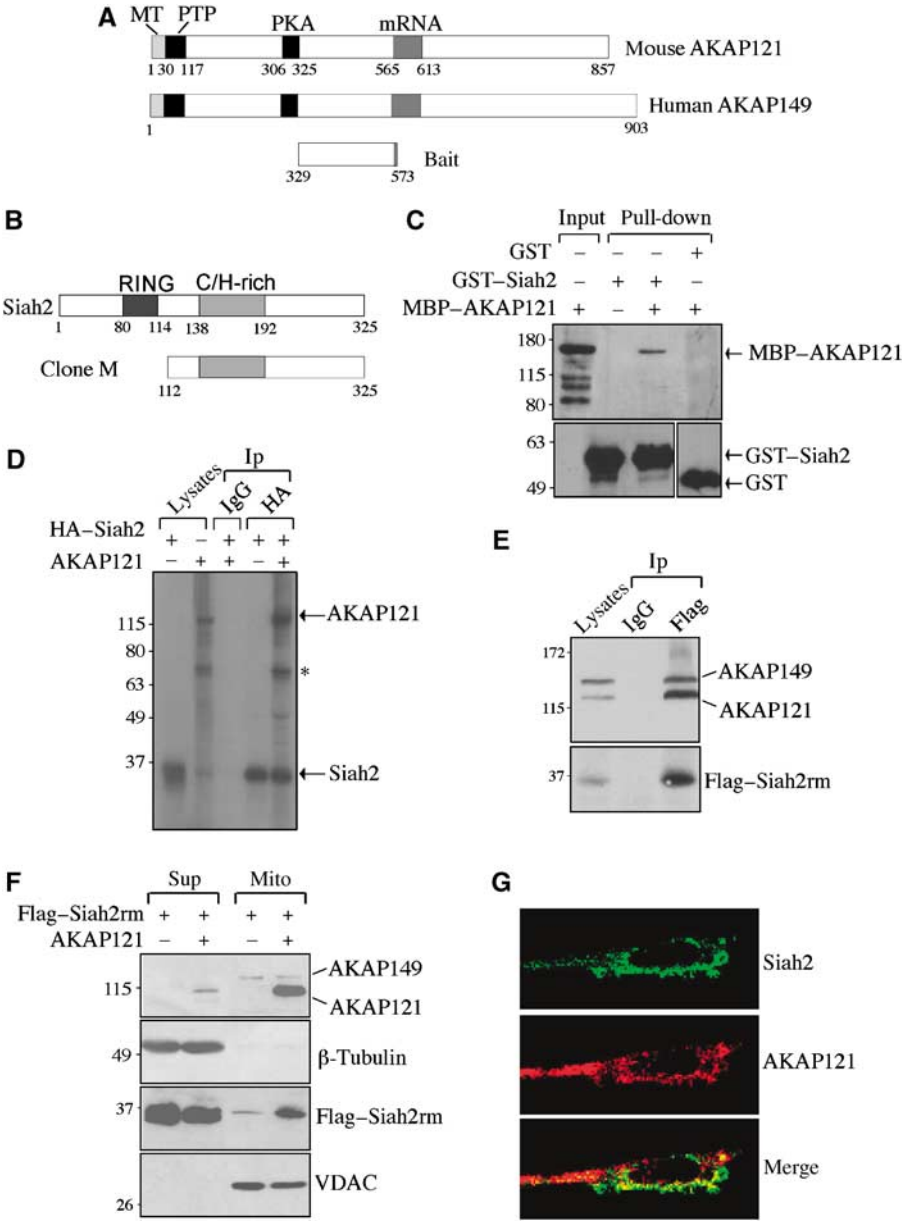

Figure 1 Siah2 binds to AKAP121. (**A**) Schematic representation of mouse AKAP121 and its human homologue AKAP149. Mitochondrial targeting motif (MT), PTPD1 (PTP), PKA R subunits and mRNA binding motifs are boxed. The AKAP121 bait (residues 329–573) was fused to the C-terminus of the DNA-binding domain of GAL4 (GAL4-BD). (**B**) Schematic representation of the clone (clone M) isolated by yeast two-hybrid analysis and its sequence homology with the C-terminus of mouse Siah2. C/H-rich, cysteine-rich region (zinc fingers); RING domain is also shown. (**C**) MBP-tagged full-length AKAP121 was incubated with purified GST-Siah2 or GST polypeptide. The bound and input fractions were immunoblotted (IB) with anti-AKAP121 (upper panel) and anti-GST (lower panel) antibodies. (**D**) *In vitro* translated, ^{35}S-labeled AKAP121 and Siah2 proteins were immunoprecipitated with anti-HA or control immune IgG. The input (1/5) and bound fractions were resolved on 10% SDS–PAGE gels. Gel was fixed, dried and exposed to X-ray film. *, small translation product. (**E**) HEK293 were transiently co-transfected with Flag–Siah2 RING mutant (Flag–Siah2$_{rm}$) and AKAP121 vectors. Twenty-four hours after transfection, cells were harvested and lysed. Lysates were subjected to immunoprecipitation with anti-Flag or control immune IgG and immunoblotted with the indicated antibodies. (**F**) Mitochondrial and supernatant fractions were isolated from HEK293 cells transiently co-transfected with AKAP121 and Siah2$_{rm}$ and immunoblotted with the indicated antibodies. A representative set of gels is shown. (**G**) Mouse fibroblasts (NIH3T3) were transiently transfected with HA-tagged Siah2 and subjected to double immunostaining for AKAP121 and HA. Images were obtained by confocal microscopy.

completely stabilized AKAP121 and AKAP149 (Figures 3A and B). In contrast to AKAP121, the three splice variants of the plasma membrane-associated AKAP-KL (105, 120 and 130 kDa) were not degraded during OGD (Figure 3A).

Neurons are highly sensitive to OGD, and their mitochondrial oxidative machinery quickly adapts to changes in fuel availability. It was of interest, therefore, to know if OGD modulated AKAP121 levels in neuronal cells. Hippocampal neurons from rat brain were subjected to OGD for 2 h. Cells were harvested and lysates analysed by immunoblotting. Figure 3C shows that OGD in hippocampal neurons, reduced AKAP121 levels by ~50%. Treatment with MG132 during

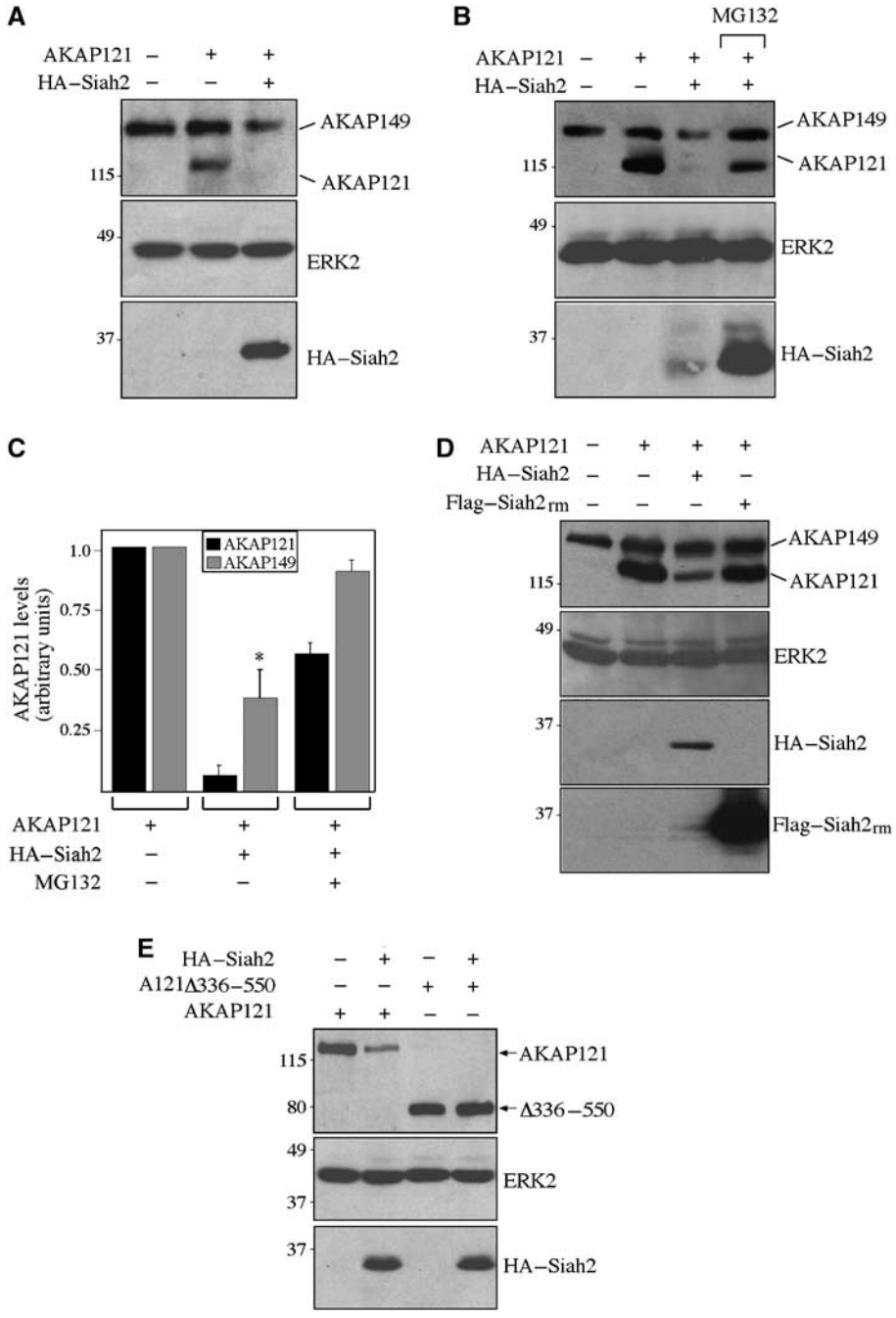

Figure 2 Siah2 promotes degradation of AKAP121. (**A**, **B**) HEK293 cells were transiently transfected with CMV, AKAP121 and HA–Siah2 expression vectors. Forty-eight hours after transfection, cells were harvested and lysed (A). Where indicated, cells were treated with MG132 (8 h), a proteasome-specific inhibitor (B). Lysates were size-fractionated on SDS–PAGE and immunoblotted with anti-AKAP121, anti-ERK2 and anti-HA antibodies. (**C**) Quantitative analysis of the experiment shown in (B). The data are indicated as mean ± s.e.m. of four independent experiments that gave similar results, and are expressed as fold decrease relative to control (AKAP121 and endogenous AKAP149, untreated cells), which was set as 1. $*P<0.05$ versus control. (**D**) Lysates from HEK293 cells transiently transfected with AKAP121 and Siah2 or $Siah2_{rm}$ were immunoblotted with the indicated antibodies. (**E**) HEK293 cells were transiently transfected with AKAP121 or $AKAP121_{\Delta 336-550}$ vectors. Where indicated, the Siah2 vector was included in the transfection mixture. Cell lysates were immunoblotted with the indicated antibodies.

OGD yielded AKAP121 levels even higher than normoxic (0 time point) cells. Similar results were seen in mouse NIH3T3 fibroblasts. Thus, AKAP121 levels fell during OGD and were restored when cells were re-exposed to glucose and oxygen for 15 h (Figure 3D).

Further evidence that Siah2 is indeed a physiological regulator of AKAP121 stability was obtained by down-regulating Siah2 expression using small interference RNA (siRNA). We used four distinct duplex siRNAs targeting distinct segments of Siah2. The constructs were transiently transfected into HEK293 or NIH3T3 cells. As controls, we used untransfected cells or cells transfected with control non-targeting siRNA ($siRNA_c$). Twenty-four hours after transfection, cells were subjected to OGD for 4 h. Figure 3E

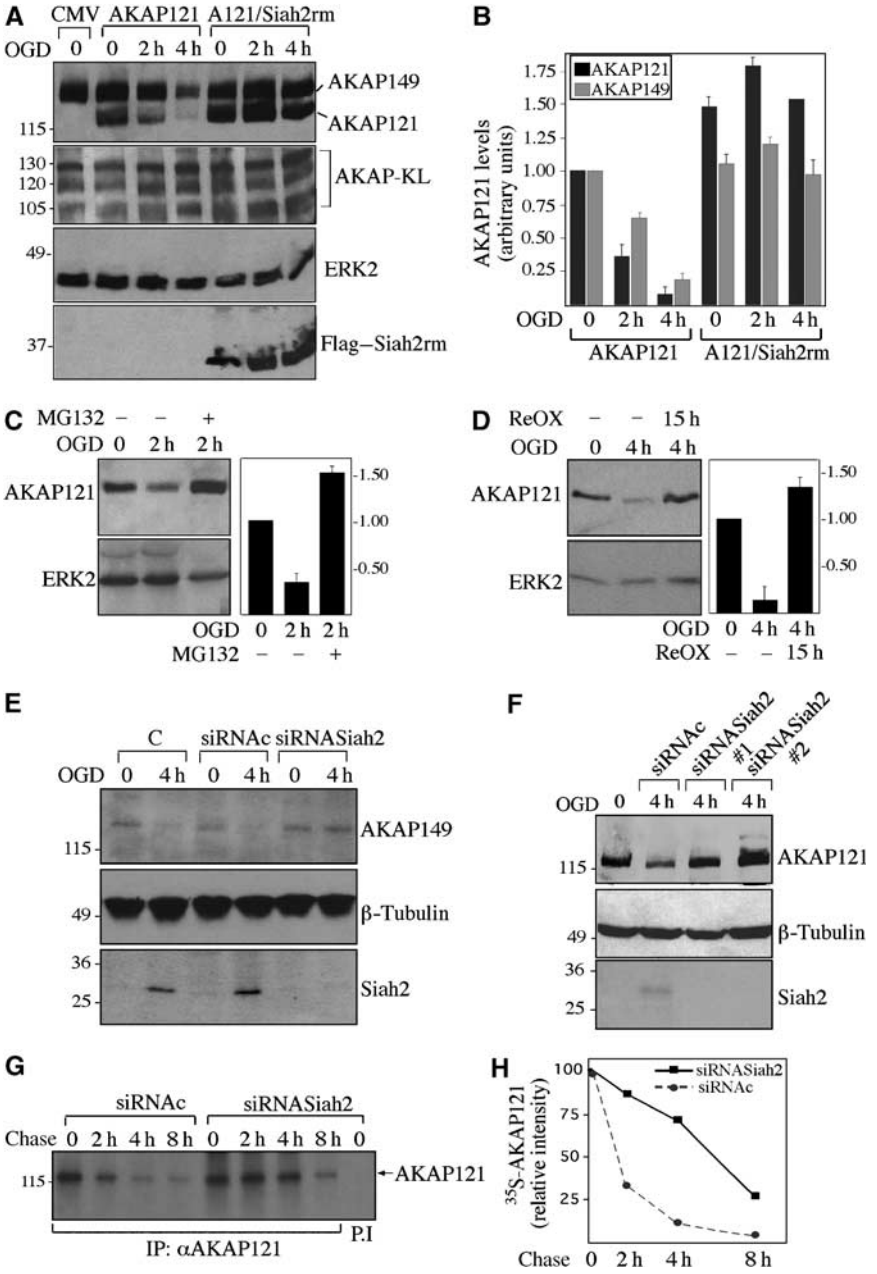

Figure 3 Oxygen and glucose deprivation (OGD) induces degradation of AKAP121 via Siah2. (**A**) HEK293 cells were transiently transfected with CMV or AKAP121 vectors. Where indicated, Flag–Siah2$_{rm}$ vector was included in the transfection mixture. Forty-eight hours after transfection, cells were either left untreated (0) or exposed to OGD. Cells were harvested at 2 and 4 h post-treatment and immunoblotted with anti-AKAP121, anti-AKAP-KL, anti-ERK2 and anti-Flag antibodies. (**B**) Quantitative analysis of the experiment shown in panel A. The data are indicated as mean of three independent experiments that gave similar results, and are expressed as fold variations ± s.e.m. relative to control (AKAP121 and endogenous AKAP149, 0 time point), which was set as 1. *, $P<0.05$ vs AKAP121 (0 time point). (**C**, **D**) Hippocampal neurons (C) or NIH3T3 mouse fibroblasts (D) were left untreated (0 time point) or subjected to OGD for 2 or 4 h. Cells were re-oxygenated (ReOX) following OGD and the medium was supplemented with glucose for additional 15 h (D) or treated during OGD with MG132 (C). Cells were harvested and protein lysates immunoblotted with anti-AKAP121 and anti-ERK2 antibodies. Cumulative data are expressed as fold variations ± s.e.m. relative to control (0 time point), which was set as 1. (**E**) HEK293 cells were transiently transfected with siRNA$_c$ or SMARTpool siRNA$_{Siah2}$ (siRNA$_{Siah2}$). Twenty-four hours following transfection, cells were either left untreated (0) or subjected to OGD (4 h). Lysates were immunoblotted with anti-AKAP121, anti-β-tubulin and anti-Siah2 antibodies. (**F**) NIH3T3 were transiently transfected with siRNA$_c$ or siRNA$_{Siah2}$ #1 or siRNA$_{Siah2}$ #2 (see Materials and methods). Twenty-four hours following transfection, cells were either left untreated (0) or subjected to OGD (4 h). Lysates were immunoblotted with anti-AKAP121, anti-β-tubulin and anti-Siah2 antibodies. (**G**) Pulse–chase experiment. Mouse fibroblasts where transfected with siRNA$_c$ or siRNAs for Siah2 (SMARTpool). Twenty-four hours later, cells were pulse-labeled for 3 h with [^{35}S]Met/Cys, chased with excess cold methionine and subjected to OGD for the indicated time points. Cell lysates were immunoprecipitated with anti-AKAP121 antibody or preimmune serum (PI) and the precipitates were subjected to autoradiography. (**H**) The data are indicated as the mean of two independent experiments shown in panel G and are expressed as fold variations relative to control (0 time point), which was set as 100.

and F shows that siRNA-mediated silencing of Siah2 abrogated OGD-induced disappearance of endogenous human AKAP149 (HEK293) and of mouse AKAP121 (NIH3T3).

Pulse–chase experiments confirmed that OGD induces degradation of newly synthesized AKAP121 in a time-dependent manner (Figures 3G and H). Downregulation of Siah2 by siRNA in OGD-treated cells decreased proteolysis of AKAP121.

As Siah2 is an E3–Ub ligase, we asked whether Siah2 modulates AKAP121 ubiquitination *in vivo*. HEK293 cells were transiently transfected with vectors encoding AKAP121 and HA-tagged Ub. Where indicated, Siah2 or its inactive RING mutant was included in the transfection mixture. Twenty-four hours following transfection, a portion of the cells was treated with the proteasome inhibitor MG132. Cells were harvested at 32 h following transfection and lysates were immunoprecipitated with anti-AKAP121 antibody. The precipitates were resolved by SDS–PAGE and immunoblotted with anti-HA antibody and AKAP121. As shown in Figure 4A, AKAP121 was, in fact, ubiquitinated *in vivo*. In the absence of MG132, most of the AKAP121 was degraded by the co-transfected Siah2, and severely reduced the accumulation of ubiquitinated AKAP121. When MG132 was added to the medium, the amount of ubiquitinated AKAP121 significantly increased in Siah2 transfected cells, compared to control or cells expressing $Siah2_{rm}$.

Next, we measured AKAP121 ubiquitination during OGD. HEK293 cells were transiently transfected with vectors encoding AKAP121 and HA-tagged Ub, in the presence or absence of siRNAs targeting Siah2 ($siRNA_{Siah2}$) or control siRNA ($siRNA_c$). Twenty-four hours following transfection, cells were subjected to OGD for 4 h and harvested. Where indicated, cells were treated with MG132 to inhibit proteasome activity. Cells were harvested 32 h post-transfection and lysates were immunoprecipitated with anti-AKAP121 antibody. Precipitates were resolved by SDS–PAGE and immunoblotted with anti-HA antibody or anti-AKAP121. Figure 4B shows AKAP121 ubiquitination under normoxic conditions. Ubiquitination was enhanced both by MG132 and by OGD treatment. Co-transfection with $siRNA_{siah2}$ drastically decreased ubiquitinated AKAP121 concentrations, compared to $siRNA_c$. This suggests that most of AKAP121 ubiquitylation *in vivo* is catalysed by Siah2.

To demonstrate that AKAP121 is a substrate of Siah2, we performed *in vitro* ubiquitination experiment using purified proteins. Figure 4C shows that recombinant Siah2 ubiquitinated *in vitro* translated, ^{35}S-labeled AKAP121.

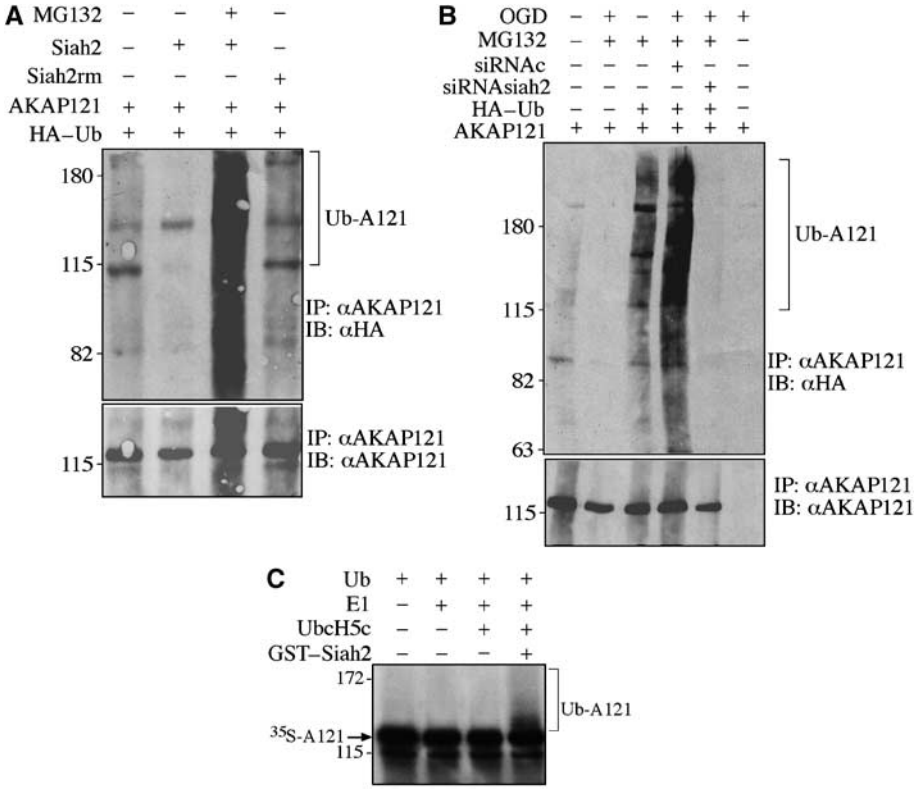

Figure 4 Hypoxia–Siah2 signalling promotes ubiquitination of AKAP121. (**A**) HEK293 cells were co-transfected with AKAP121 and HA-tagged ubiquitin. Where indicated, vectors encoding Siah2 or $Siah2_{rm}$ were included in the transfection mix. Twenty-four hours after transfection, cells were treated with MG132 (20 μM) for an additional 8 h. Lysates were then prepared, immunoprecipitated with anti-AKAP121 and immunoblotted with anti-HA antibodies. (**B**) HEK293 cells were co-transfected with AKAP121 and HA-tagged ubiquitin. Where indicated, control ($siRNA_c$) or SMARTpool $siRNA_{Siah2}$ ($siRNA_{siah2}$) was included in the transfection mix. Twenty-four hours after transfection, cells were subjected to OGD for 4 h in the presence or absence of MG132, and lysed. Lysates were immunoprecipitated with anti-AKAP121 and immunoblotted with anti-HA and anti-AKAP121 antibodies. (**C**) *In vitro* translated and ^{35}S-labeled AKAP121 was incubated with purified GST–Siah2 and His_6-tagged ubiquitin in the presence or absence of E1, UbcH5c (E2) and at 37°C for 45 min. The reaction mix was denatured, size-fractionated by 7% SDS–PAGE and analysed by autoradiography.

Siah2 affects mitochondrial activity

We previously showed that AKAP121 enhances $\Delta\Psi_m$ and oxidative ATP synthesis by directing PKA and src signalling to mitochondria (Livigni *et al*, 2006). To further investigate these interactions, we generated AKAP121 deletion mutants that lack either the PKA or the PTPD1/src-binding domain. Figure 5A shows that transfection of HEK293 cells with wild-type AKAP121 enhanced $\Delta\Psi_m$, whereas transfection with AKAP121 mutants that fail to bind PKA ($AKAP121_{L313,\ 319P}$) or PTPD1/src ($AKAP121_{\Delta45-110}$) decreased $\Delta\Psi_m$. Note that $AKAP121_{L313,\ 319P}$ reduced $\Delta\Psi_m$ more severely than $AKAP121_{\Delta45-110}$. This mutant was potently proapoptotic when expressed in cultured rat pheochromocytoma PC12 cells (Affaitati *et al*, 2003).

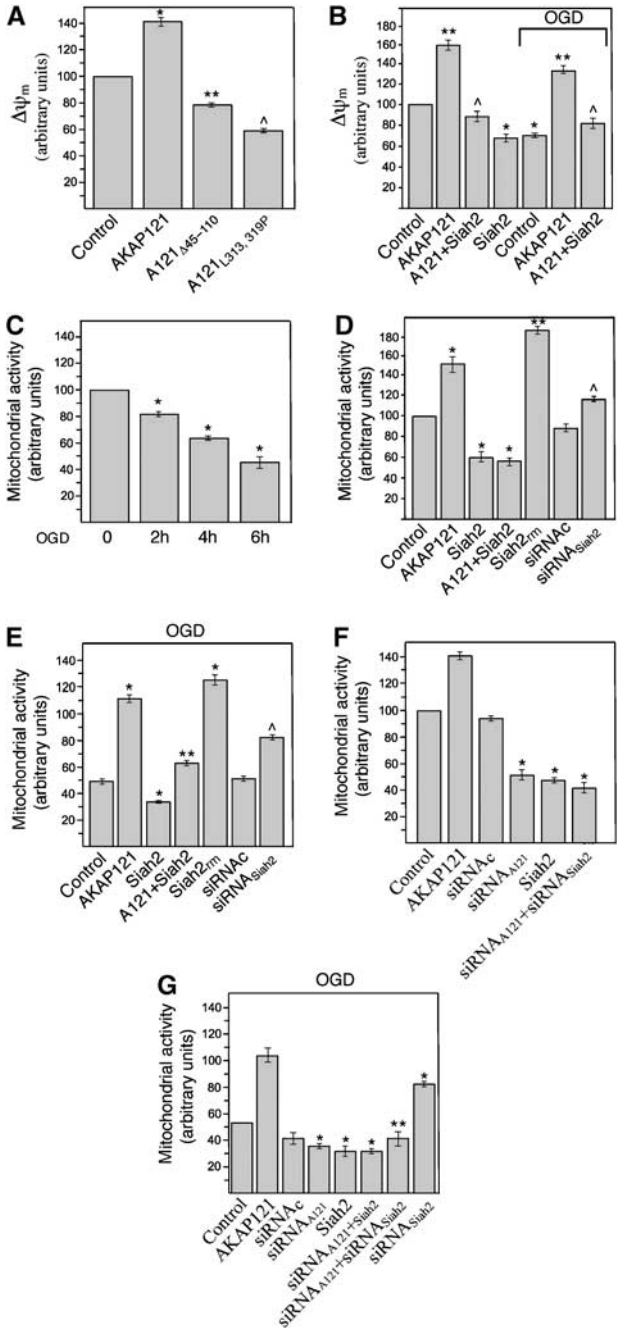

We next asked if degradation of AKAP121 promoted by OGD or Siah2 affected the mitochondrial oxidative machinery. Expression of Siah2 reduced basal $\Delta\Psi_m$ levels and abolished stimulation by AKAP121 (Figure 5B). As expected, OGD lowered $\Delta\Psi_m$ in control cells. Notably, cells transfected with AKAP121 maintained their $\Delta\Psi_m$ in the face of OGD. Siah2 coexpression reversed the resistance to OGD promoted by AKAP121.

Next, we assessed mitochondrial oxidative capacity by the 3-(4,5-dimethylthiazol-2-yl)-2,5, diphenyltetrazolium bromide (MTT) assay in which MTT tetrazolium dye is reduced to a dark blue formazan precipitate by active mitochondrial succinate dehydrogenase. Figure 5C shows that OGD treatment decreased mitochondrial activity in a time-dependent manner. These effects paralleled the time-dependent degradation of AKAP121 during OGD (see Figure 3; Supplementary Figure S1). Next, we evaluated whether Siah2 affects mitochondrial activity. Figure 5D shows that expression of AKAP121 or the Siah2 ring mutant ($Siah2_{rm}$) increased MTT by ~40 and ~70%, respectively. In contrast, Siah2 expression decreased MTT by ~40%, even in presence of coexpressed AKAP121. Treatment with $siRNA_{Siah2}$ slightly, but reproducibly, increased mitochondrial activity.

We determined whether AKAP121 and Siah2 modulate mitochondrial metabolic activity during OGD. The results are summarized in Figure 5E. OGD impaired mitochondrial metabolic activity by ~50%. This decrease was reversed by transfection with AKAP121. Expression of Siah2 further

Figure 5 Regulation of mitochondrial membrane potential ($\Delta\Psi_m$) and dehydrogenase activity (MTT) by AKAP121 and Siah2. (**A**) TMRE analysis of HEK293 cells transiently co-transfected with GFP and CMV or AKAP121 expression vectors (AKAP121, $AKAP121_{\Delta45-110}$, $AKAP121_{L313,\ 319P}$). Cumulative data are expressed as mean ± s.e. of changes in TMRE fluorescence and represent fold increase over control (CMV) cells, which was set as 100. The intensity of fluorescence was evaluated in single cells with Meta Morph software analysis. $^*P<0.05$ versus CMV-transfected (GFP positive) cells; $^{**}P<0.05$ versus AKAP121-transfected (GFP positive) cells; $^\wedge P<0.05$ versus CMV-transfected (GFP positive) cells. Statistical analysis was performed by ANOVA and Newman–Keuls methodology. (**B**) TMRE analysis of HEK293 cells transiently co-transfected with GFP and the indicated vectors, left untreated or exposed to OGD for 4 h before harvesting. Cumulative data are expressed as mean ± s.e.m. of changes in TMRE fluorescence and represent fold increase over control (CMV, untreated cells), which was set as 100. $^*P<0.05$ versus CMV-transfected (GFP positive) cells; $^{**}P<0.05$ versus CMV-, CMV/OGD- and Siah2-transfected (GFP positive) cells; $^\wedge P<0.05$ versus AKAP121- and AKAP121/OGD-transfected (GFP positive) cells. (**C**) MTT assay in HEK293 cells transiently transfected with AKAP121. Twenty-four hours after transfection, cells were harvested and mitochondrial dehydrogenase activity was assayed as described under Materials and methods. $^*P<0.02$ versus each preceding time point. (**D**) MTT assay in HEK293 cells transiently transfected with the indicated vectors. $^*P<0.05$ versus control; $^{**}P<0.05$ versus AKAP121-transfected cells; $^\wedge P<0.05$ versus $siRNA_c$-transfected cells. (**E**) Same as in panel D, except that cells were subjected to OGD for 4 h before harvesting. $^*P<0.05$ versus control, $^{**}P<0.05$ versus control and AKAP121-transfected cells; $^\wedge P<0.05$ versus control and $siRNA_c$-transfected cells. (**F**, **G**) MTT assay in HEK293 cells transiently transfected with the following vectors: empty vector (control), AKAP121, Siah2, control siRNA ($siRNA_c$), $siRNA_{AKAP121}$ and SMARTpool $siRNA_{Siah2}$ ($siRNA_{Siah2}$). $siRNA_{AKAP121}$ vector was described previously (Livigni *et al*, 2006). Twenty-four hours following transfection, cells were left untreated (F) or subjected to OGD (G) for 4 h before harvesting. $^*P<0.02$ versus control; $^{**}P<0.05$ versus control.

decreased MTT levels by ~30% and mostly abolished the protective effects of AKAP121. In contrast, $Siah2_{rm}$ completely restored mitochondrial oxidative activity in OGD-treated cells. To prove further that Siah2 indeed decreased mitochondrial metabolic capacity during hypoxia, we performed MTT assays in cells transfected with $siRNA_{Siah2}$. As shown in Figure 5E, transfection with $siRNA_{Siah2}$ increased mitochondrial metabolic activity in OGD-treated cells (~80% of non transfected, normoxic cells), compared with $siRNA_c$-transfected cells.

To establish a mechanistic link between downregulation of AKAP121 and MTT changes in cells exposed to OGD or Siah2, we measured mitochondrial activity in cells in which AKAP121 was eliminated by RNA interference. Figures 5F and G show that downregulation of AKAP121 significantly decreased MTT. Similar effects were observed when both AKAP121 and Siah2 were downregulated. During OGD, elimination of Siah2 by $siRNA_{siah2}$ partly restored MTT, whereas concomitant downregulation of AKAP121 by $siRNA_{A121}$ suppressed $siRNA_{siah2}$'s effects.

Middle cerebral artery occlusion induces AKAP121 degradation

We next determined AKAP121 levels in several brain regions following permanent middle cerebral artery occlusion (pMCAO). This procedure induces ischaemic damage of the frontal cortex without affecting the hippocampus. Rat brains subjected to pMCAO were isolated and dissected. AKAP121 levels were analysed by immunofluorescence in the ischaemic core (PC1), in the area surrounding the ischaemic core (PC2) and in the hippocampus ipsilateral and contralateral to the lesion. Figures 6A and B show that AKAP121 immunoreactivity was reduced by 85% in the ischaemic core compared with levels detected in the contralateral hemisphere and in sham-operated animals. In contrast, AKAP121 expression was unaffected in the area surrounding the ischaemic core. Interestingly, levels of AKAP121 protein were statistically higher in the CA1 region of the hippocampus ipsilateral to the ischaemic lesion as compared with those detected in the contralateral hemisphere and in sham-operated rat. Moreover, AKAP121 decreases progressively from the ischaemic core to the perinfarct area (Supplementary Figure S2). AKAP121 in the surviving neurons gradually disappears in neurons that are closer or within the ischaemic core.

To evaluate whether the difference in AKAP121 protein expression detected during ischaemia occurred in neurons or in other cell types, we performed a double immunofluorescence staining for AKAP121 and neuronal nuclei (NeuN), a neuron-specific nuclear protein marker (Mullen *et al*, 1992). Figure 7A shows that AKAP121 was expressed in all NeuN-positive neuronal cells. The number of NeuN-positive cells was reduced by ~40% in the core region and the surviving NeuN-positive neurons showed intact morphological properties (Figure 7B). In approximately 35% of surviving NeuN-positive neurons AKAP121 immunoreactivity was absent (Figure 7C). These findings confirm that AKAP121 was downregulated in several neurons of the core region of ischaemic brain. The loss of AKAP121 during brain ischaemia was also documented by western blot analysis of protein lysates from control and ischaemic rat brain (Figure 8A and B).

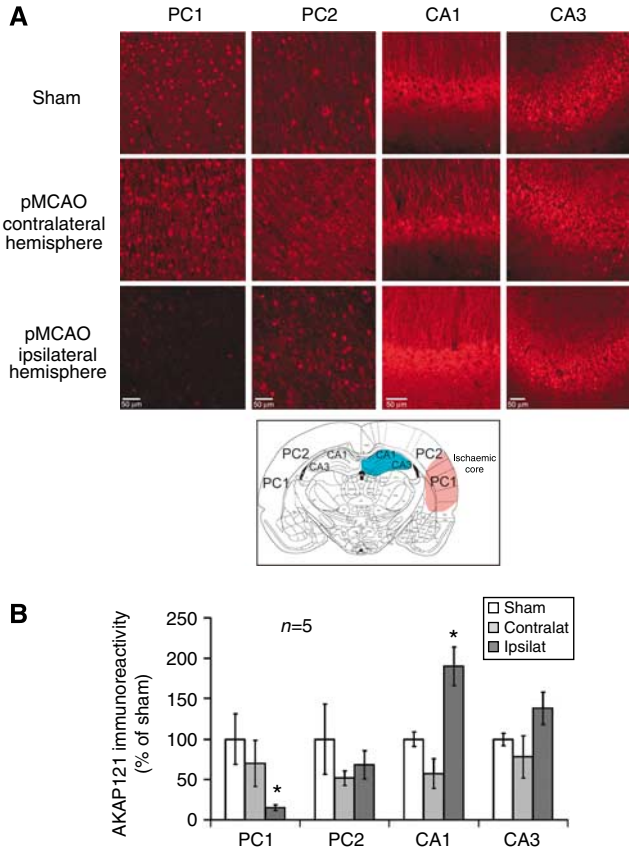

Figure 6 AKAP121 disappears during cerebral ischaemia. (**A**) Brain sections from rats subjected to pMCAO include parietal cortical (PC1 and PC2) and hippocampal (CA1 and CA3) areas isolated from the ischaemic ispilateral hemisphere and from the non-ischaemic contralateral hemisphere. Sections from sham-operated rats were used as controls. Brain sections were immunostained with anti-AKAP121 antibody and analysed by confocal microscopy. (**B**) Quantitative analysis of the AKAP121 immunoreactivity from rat brain subjected to pMCAO. Fluorescence intensity was measured by using ImageJ 1.38 software. The data are expressed as percent of fluorescence intensity ± s.e.m. compared with sham-operated controls. Statistical analysis was performed using separated one-way ANOVAs for each region and *post hoc* repeated-measure comparisons (LSD test). Rejection level was set at $P<0.01$. $^*P<0.01$ versus contralateral and sham-operated groups.

To link AKAP121 disappearance to Siah2 signaling, siRNA targeting Siah2 ($siRNA_{siah2}$) or control siRNA ($siRNA_c$) were intracerebroventricularly (icv) perfused in sham-operated rats or subjected to pMCAO. Intracerebral infusion of siRNAs targeting Siah2 caused reduction of Siah2 protein in the perfused hemisphere (data not shown). Figure 8C shows that icv treatment with $siRNA_{siah2}$ prevented degradation of AKAP121 in the PC1 core region of the ischaemic hemisphere.

Discussion

We have identified a novel mechanism by which the cell, in response to reduction in oxygen availability, degrades mitochondrial scaffold protein AKAP121. AKAP121 transmits both cAMP/PKA and EGF/src signals to mitochondria, thus stimulating ATP synthesis. Hypoxia-induced E3–Ub ligase Siah2 was detected in complex with AKAP121. Siah2 binding leads to ubiquitination and rapid degradation of AKAP121,

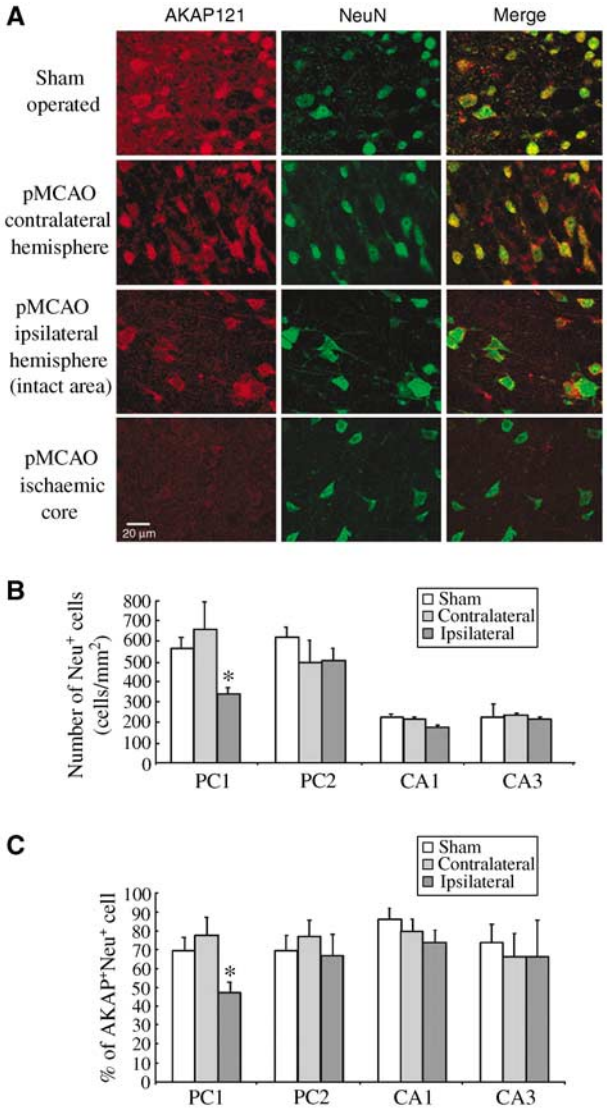

Figure 7 Sections from control or ischaemic parietal cortex include ischaemic core (PC1) and non-ischaemic parietal cortex (PC2) from the ispilateral hemisphere, PC1 from the contralateral hemisphere and PC1 from sham-operated rats. (**A**) Sections were doubly immunostained with anti-AKAP121 and anti-NeuN antibodies, and analysed by confocal microscopy. (**B**) Quantitative analysis of NeuN-positive cells from the ischaemic core (PC1), the area surrounding the ischaemic core (PC2) and the hippocampus (CA1 and CA3) of the ipsilateral and contralateral hemispheres. (**C**) LSD multiple-comparison test between AKAP121-positive and NeuN-positive cells. Values are expressed as percentage of AKAP121-positive cells calculated as follows: % $AKAP^+$ cells = (number of $AKAP^+$ $NeuN^+$ cells)/(number of $NeuN^+$ cells) × 100).

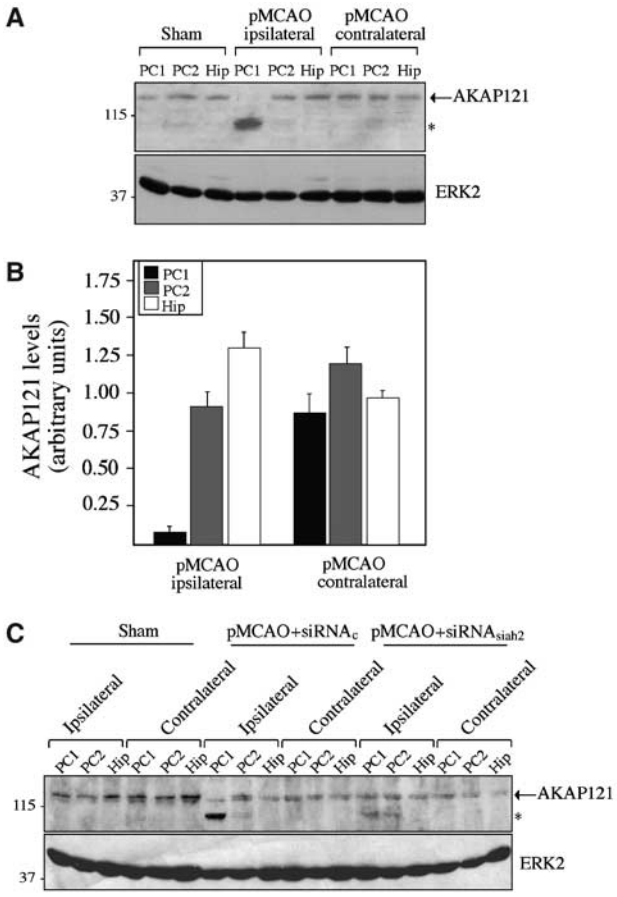

Figure 8 Siah2 is required for AKAP121 disappearance in ischaemic rat brain. (**A**) Immunoblot analysis of lysates from PC1, PC2 and hippocampus (Hip) of ischaemic, contralateral and sham-operated hemispheres from the rat brain. (**B**) Cumulative data are expressed as mean ± s.e.m. of three independent experiments that gave similar results. The values are relative to the same areas of sham animals that were set as 1. (**C**) Rat brains were perfused with control ($siRNA_c$) or SMARTpool $siRNA_{Siah2}$ ($siRNA_{Siah2}$), and 12 h later were subjected to pMCAO. Lysates were immunoblotted with the indicated antibody. A representative experiment is shown. In this set of experiments, the antibody directed against residues 200–450 of mouse AKAP121 (see Materials and methods) detected an AKAP121 degradation product (*) that specifically accumulated in ischaemic PC1.

both *in vitro* and in intact tissue. The consequent drop in AKAP121 concentrations significantly reduced mitochondrial activity.

In higher eukaryotes, oxygen fuels mitochondrial respiration and oxidative ATP synthesis. Oxygen concentration is maintained at physiological levels by highly organized respiratory and circulatory systems. In ischaemia, obstruction of blood flow to tissue leads to decrease of oxygen (hypoxia) and metabolite diffusion to cells. Hypoxia is rapidly detected by oxygen-sensing mechanisms that alter gene transcription patterns. These alterations have an important role in switching from oxidative to fermentative metabolism.

The major regulator of cellular responses to hypoxia is HIF1α. HIF-1α is a transcription factor composed of a heterodimer of a hypoxia-inducible α-subunit and a constitutively expressed β-subunit. HIF-1α induces expression of a number of genes, including that of vascular endothelial growth factor, transforming growth factor-β and erythropoietin, which are involved in vascularization, erythropoiesis, metabolism and other central cellular processes. Under normoxic conditions, HIF-1α hydroxylation by PHD2 promotes HIF-1α binding to the von Hippel–Lindau complex and rapid degradation by the Ub–proteasome pathway (Berra *et al*, 2003). Hypoxia induces expression of Siah2, which carries an N-terminal RING domain followed by two zinc-finger motifs and a C-terminal substrate-binding domain. The RING finger domain of Siah2 mediates transfer of Ub monomer from E2 Ub–ligase to PHD1/3, promoting its proteasomal degradation. As a result,

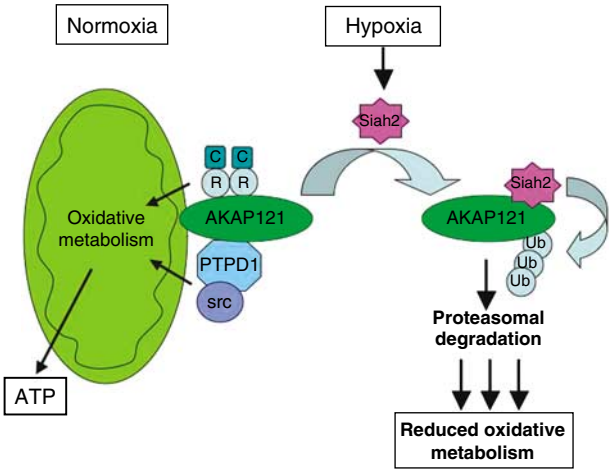

Figure 9 AKAP121 assembles a PKA and PTPD1/src-signalling complex on mitochondria that is required for oxidative metabolism and ATP synthesis. Hypoxia induces Siah2 accumulation. The E3 Ub–ligase binds to and ubiquitinates AKAP121, leading to proteasomal degradation of the anchor protein and consequent decrease of oxidative metabolism.

HIF-1α accumulates and activates transcription of hypoxia-induced genes (Hu *et al*, 1997; Nakayama *et al*, 2004).

We report here that cells also utilize another mechanism to adapt physiologically to oxygen deprivation. This involves regulation of components of the signal transduction pathway that controls oxidative respiration at the post-translational level. Our findings demonstrate that Siah2 induces ubiquitination and proteasomal degradation of the scaffold protein AKAP121, thus lowering the basal activity of mitochondrial respiration in hypoxic cells. Given its role in mitochondrial physiology, changes of AKAP121 abundance are expected to have a major impact on signalling to mitochondria (Feliciello *et al*, 2005). Indeed, we found that in hypoxic cells or cells overexpressing Siah2, AKAP121 degradation was accompanied by a significant decrease in $\Delta\Psi_m$ and mitochondrial metabolic activity. Loss of AKAP121 was quite rapid, occurring in hypoxic cells within 2–4 h of hypoxia onset. Downregulation of AKAP121 in hypoxic conditions is not cell-specific, as we detected it in fibroblasts, human embryonic kidney cells and hippocampal neurons. We also observed loss of AKAP121 in ischaemic rat brain. AKAP121 is expressed in discrete brain areas, including hippocampus and cortex, as well as in the corpus striatum and cerebellum. Middle cerebral artery occlusion consistently decreased AKAP121 levels specifically in the ischaemic cortical area. Perfusing rat brain with siRNA that targeted Siah2 prevented AKAP121 disappearance, suggesting that Siah2 was responsible for AKAP121 downregulation during brain ischaemia.

In summary, we have demonstrated a new mechanism by which cells and tissues rapidly adapt the oxidative pathway to a drop in oxygen availability. Degradation of mitochondrial AKAP121 by the hypoxia–Siah2–proteasome pathway attenuates mitochondrial respiration and oxidative ATP synthesis (see Figure 9). In view of the ubiquitous expression of AKAP121, this regulatory system might likely be used as a rapid and efficient way to attenuate oxidative metabolism during hypoxia in most, if not all, tissues.

Materials and methods

Cell lines

The human embryonic kidney cell line HEK293 and NIH3T3 cells were cultured in Dulbecco's modified Eagle's medium (DMEM) containing 10% foetal calf serum in an atmosphere of 5% CO_2. Where indicated, cells were propagated in DMEM medium supplemented with 10% calf serum. Hippocampal neurons were prepared from 18-day-old rat embryos (Irace *et al*, 2005). Neurons were cultured at 37°C in a humidified 5% CO_2 atmosphere, with medium replenishment after 6 days, and used after 11 days of culture in all experiments.

Animals

Male Wistar rats (Charles River, Lecco, Italy) were housed under diurnal lighting conditions (12-h darkness and 12-h light) and fasted overnight, but were allowed free access to water before the experiment. Experiments were performed according to international guidelines for animal research and the experimental protocol was approved by the Animal Care Committee of the University of Naples.

Plasmids and transfection

Mouse pCEP4-AKAP121 cDNA was a gift from Dr C Rubin (Albert Einstein College of Medicine, NY). Vectors encoding the Siah2 and $Siah2_{rm}$ mutants were described previously (Nakayama *et al*, 2004). HA-tagged ubiquitin was provided by Dr Antonio Leonardi (University of Naples, Italy); pcDNA3.1 vector carrying V5/His-tagged AKAP121, pCEP4-$AKAP121_{\Delta 336-550}$ vector and pCEP4–$A121_{\Delta 45-110}$ mutant were generated by PCR using specific oligo primers; pMAL-AKAP121 vector encoding MBP–AKAP121 fusion and the AKAP121 mutant lacking PKA-binding activity ($AKAP121_{L313,\ 319P}$) were described previously (Ginsberg *et al*, 2003; Affaitati *et al*, 2003).

siGENOME duplex siRNAs and siGENOME SMART pool targeting four distinct segments of Siah2 were purchased from Dharmacon. We used three different $siRNA_{Siah2}$ mixtures, (a) $siRNA_{Siah2}$ SMARTpool, containing equimolar concentrations of all four duplex siRNAs; (b) $siRNA_{Siah2}$ #1, containing equimolar concentrations of two duplex siRNAs (D-041993-01, D-041993-02) and (c) $siRNA_{Siah2}$ #2, containing equimolar concentrations of two duplex siRNAs (D-041993-03 and D-041993-04). The siRNAs were transiently transfected using Lipofectamine 2000 (Invitrogen) at a final concentration of 250 pmol/ml of culture medium.

Antibodies and chemicals

Goat polyclonal antibodies directed against AKAP121 (C-20), VDAC and Siah2, and mouse anti-ERK2 antibody were purchased from Santa Cruz Biotechnology; anti-HA epitope (HA.11) from Covance; anti-tubulin from Sigma; anti-NeuN monoclonal antibody from Chemicon International (CA, USA). Anti-AKAP KL antibody was a gift from Dr C Rubin. A polyclonal antibody directed against AKAP121 was raised as follows. A polypeptide segment spanning residues 200–450 of mouse AKAP121, expressed and purified from BL21, was used to immunize rabbit. The specificity of the antibody was tested by immunoprecipitation, immunoblot analysis and immunodepletion assays (Supplementary Figure S3).

Pulse–chase experiments

Cells were washed and incubated for 1 h in Met/Cys-free DMEM. Labelling was performing for 3 h with DMEM supplemented with [^{35}S]Met/Cys (100 μCi/ml, 1000 Ci/mmol). Cells were then washed with non-radioactive medium, incubated in serum-supplemented DMEM and cold excess methionine, and harvested (chase) for the indicated time period. Cell lysates were immunoprecipitated with anti-AKAP121 antibody, size-fractionated by 8% SDS–PAGE and subjected to autoradiography. AKAP121 signal was quantified by a PhosphorImager (Molecular Dynamics).

Immunoprecipitation and immunoblot analysis

Cells were homogenized and subjected to immunoprecipitation and immunoblot analyses as described previously (Livigni *et al*, 2006). Cytosolic and mitochondrial fractions were isolated as indicated previously (Hovius *et al*, 1990). Chemiluminescence (ECL) signals were quantified by scanning densitometry (Molecular Dynamics). ^{35}S-labeled AKAP21 and HA-tagged Siah2 were synthesized *in vitro*

using the TnT quick coupled transcription/translation system (Promega) in the presence of 45 μCi of [^{35}S]Met and Cys. The reaction mixture was subjected to immunoprecipitation with anti-HA or control IgG antibody. Precipitates were resolved by 8% SDS–PAGE and visualized by autoradiography.

Pull-down assay

MBP–AKAP121 and GST–Siah2 were expressed in Bl21 (DE3) pLysS cells and purified as previously described (Ginsberg *et al*, 2003; Cardone *et al* 2004). A 20-μl volume of GST–Siah2 beads was incubated with 1 μg of recombinant MBP-tagged AKAP121 polypeptides in 200 μl PBS1X containing 0.5% Triton X-100 with rotation at 4°C for 3 h. Pellets were washed four times in binding buffer and eluted in Laemmli buffer. The eluted samples were resolved on 8% PAGE gel, transferred to polyvinylidene difluoride membranes and immunoblotted with anti-GST or anti-AKAP121 antibodies.

In vitro ubiquitination assay

^{35}S-labeled AKAP21 was synthesized *in vitro* using the TnT quick coupled transcription/translation system (Promega) in the presence of 45 μCi of [^{35}S]Met. The ubiquitination assay was performed in buffer containing 50 mM Tri–HCl, pH 8, 0.5 mM dithiothreitol, phosphatase and protease inhibitors, supplemented with recombinant His–Ub (0.5 μg), 2 mM ATP, E1 (0.5 μg) (Affinity Research, Exeter, UK), purified E2 (0.5 μg) (UbcH5b) in the presence or absence of GST–Siah2. The reaction mixture was incubated at 37°C for 45 min; then the reaction was stopped with Laemmli buffer and the mixture was size-fractionated by 7% SDS–PAGE. Ubiquitination products were visualized by autoradiography.

MTT assay

Mitochondrial activity was assessed by measuring the level of mitochondrial dehydrogenase activity using the reduction of MTT as the substrate (Hansen *et al*, 1989; Scorziello *et al*, 2004).

Mitochondrial membrane potential

Mitochondrial membrane potential ($\Delta\Psi_m$) was assessed using the fluorescent dye tetramethyl rhodamine ethyl ester (TMRE) in the 'redistribution mode' as described previously (Livigni *et al*, 2006). Confocal images were obtained using a Zeiss inverted 510 confocal laser-scanning microscope and a ×63 oil-immersion objective. The illumination intensity of 543 mm xenon laser, used to excite TMRE fluorescence, was kept to a minimum (0.5%) of laser output in order to avoid phototoxicity.

Combined OGD

Hippocampal neurons and HEK293 cells were exposed to OGD for 3 h according to a previously reported protocol (Goldberg and Choi 1993). Re-oxygenation was achieved by returning cell cultures to normoxic conditions (37°C in a humidified 5% CO_2 atmosphere) for 24 h.

Permanent middle cerebral artery occlusion

pMCAO was performed as described previously (Pignataro *et al*, 2004). Twenty-four hours after pMCAO, the animals were perfused with paraformaldehyde (4%) and then decapitated to remove the brains. Sham-operated controls underwent surgical procedures except for electrocoagulation of the middle cerebral artery. The brain was placed on dry ice and the coronal sections were cut with a vibratome (752M; Campden Instrument, London, UK).

siRNA administration in rat brain

All rats, anesthetized with chloral hydrate (400 mg/kg, intraperitoneally), were put on a stereotaxic frame. A 23-G stainless steel guide cannula (Small Parts Inc., Miami Lakes, FL) was implanted into the right lateral ventricle, the third ventricle, using stereotaxic coordinates of 0.5 mm caudal to bregma, 2 mm lateral and 2.5 mm below the dura. The cannula was fixed to the cranium using dental acrylic and small screws. siRNAs targeting Siah2 (pool #2) (10 μl from 250 μM stock) and control siRNAs (10 μl from 250 μM stock) were administered three times, 24 and 6 h before ischaemia induction and just after pMCAO. AKAP protein expression was analysed 24 h after ischaemia onset.

Confocal immunofluorescence analysis

Forebrain coronal vibratome sections were subjected to immunostaining with incubated anti-AKAP121 and anti-NeuN antibodies. Immunofluorescence was visualized using a Zeiss LSM 510 Meta argon/krypton laser-scanning confocal microscope. Four images from each optical section were averaged to improve the signal to noise ratio.

Image analysis

A minimum of four sections per brain and four different samples per region were analysed. For each image, the average grey level in a region of interest was quantified along with the background grey level using ImageJ 1.38 software. Signals were background-subtracted and expressed as percent of sham control. To evaluate whether changes in AKAP expression were dependent on changes in the number of neurons, we calculated the total number of neurons per unit area in each Region of Interest (ROI) using NeuN as marker, and within each region counted the number of AKAP-positive cells. We compared the number of AKAP-positive and NeuN-positive cells with the total number of NeuN-positive cells and expressed this value as percentage of AKAP-positive cells (%AKAP+ = (number of $AKAP^+$ $NeuN^+$ cells)/(number of $NeuN^+$ cells) × 100).

Statistics

Image analysis data were analysed using separated one-way analysis of variance (ANOVA) for each region and *post hoc* repeated-measure comparisons (Least Significant Difference (LSD) test). Rejection level was set at $P<0.01$. MTT results are expressed as mean±s.e.m. Statistical analysis was performed by using ANOVA test followed by Newman–Keuls test. $P<0.05$ was considered statistically significant.

Supplementary data

Supplementary data are available at *The EMBO Journal* Online (http://www.embojournal.org).

Acknowledgements

This work was supported by grant from 'Associazione Italiana per la Ricerca sul Cancro' (AIRC). AF was partly supported by 'UICC American Cancer Society Beginning Investigators Fellowship funded by the American Cancer Society', and the 'Italian Academy for Advanced Studies in America' NY. LA was supported by grants from the Italian Ministry of Health 'Programma Speciale art. 12 bis comma 6, D. Lgs. 229/99 and COFIN 2006'. Special thanks to Dr Z Ronai (BIMR, La Jolla, CA USA) for providing Siah2/Siah2rm expression vectors, to Dr C Rubin (Albert Einstein College of Medicine) for mouse AKAP121 vector and anti-AKAP-KL antibody, and to Dr S Goff (Columbia University, NY) for the pGAD cDNA library. This work is dedicated to the memory of Francesca Graziano.

References

Affaitati A, Cardone L, Carlucci A, de Cristofaro T, Ginsberg MD, Varrone S, Gottesman ME, Avvedimento VE, Feliciello A (2003) Essential role of A-kinase anchor protein 121 for cAMP signalling to mitochondria. *J Biol Chem* **278:** 4286–4294

Barman AL, Soughayer J, Nguyen BT, Willoughby D, Carnegie GK, Wong W, Hoshi N, Langeberg LK, Cooper DM, Dessauer CW, Scott JD (2006) Dynamic regulation of cAMP synthesis through anchored PKA–adenylyl cyclase V/VI complexes. *Mol Cell* **23:** 925–931

Berra E, Benizri E, Ginouvès A, Volmat V, Roux D, Pouysségur J (2003) HIF prolyl-hydroxylase 2 is the key oxygen sensor setting low steady-state levels of HIF-1alpha in normoxia. *EMOB J* **22:** 4082–4090

Boehm J, He Y, Greiner A, Staudt L, Wirth T (2001) Regulation of BOB.1/OBF.1 stability by SIAH. *EMBO J* **20:** 4153–4162

Cardone L, Carlucci A, Affaitati A, Livigni A, DeCristofaro T, Garbi C, Varrone S, Ullrich A, Gottesman ME, Avvedimento EV, Feliciello A (2004) Mitochondrial AKAP121 binds and targets

protein tyrosine phosphatase D1, a novel positive regulator of src signalling. *Mol Cell Biol* **24:** 4613–4626

Chavez JC, Baranova O, Lin J, Pichiule P (2006) The transcriptional activator hypoxia inducible factor 2 (HIF-2/EPAS-1) regulates the oxygen-dependent expression of erythropoietin in cortical astrocytes. *J Neurosci* **26:** 9471–9481

Chen Q, Lin RY, Rubin CS (1997) Organelle-specific targeting of protein kinase AII (PKAII). Molecular and *in situ* characterization of murine A kinase anchor proteins that recruit regulatory subunits of PKAII to the cytoplasmic surface of mitochondria. *J Biol Chem* **272:** 15247–51527

Dell'Acqua ML, Smith KE, Gorski JA, Horne EA, Gibson ES, Gomez LL (2006) Regulation of neuronal PKA signaling through AKAP targeting dynamics. *Eur J Cell Biol* **85:** 627–633

Feliciello A, Gottesman ME, Avvedimento EV (2001) The biological functions of A-kinase anchor proteins. *J Mol Biol* **308:** 99–114

Feliciello A, Gottesman ME, Avvedimento EV (2005) cAMP–PKA signalling to the mitochondria: protein scaffolds, mRNA and phosphatases. *Cell Signal* **17:** 279–287

Feliciello A, Li Y, Avvedimento EV, Gottesman ME, Rubin CS (1997) A-kinase anchor protein 75 increases the rate and magnitude of cAMP signalling to the nucleus. *Curr Biol* **7:** 1011–1014

Feliciello A, Rubin CS, Avvedimento VE, Gottesman ME (1998) Expression of A kinase anchor protein 121 is regulated by hormones in thyroid and testicular germ cells. *J Biol Chem* **273:** 23361–23366

Frew IJ, Hammond VE, Dickins RA, Quinn JM, Walkley CR, Sims NA, Schnall R, Della NG, Holloway AJ, Digby MR, Janes PW, Tarlinton DM, Purton LE, Gillespie MT, Bowtell DD (2003) Generation and analysis of Siah2 mutant mice. *Mol Cell Biol* **23:** 9150–9161

Ginsberg MD, Feliciello A, Jones JK, Avvedimento EV, Gottesman ME (2003) PKA-dependent binding of mRNA to the mitochondrial AKAP121 protein. *J Mol Biol* **327:** 885–897

Goldberg MP, Choi DW (1993) Combined oxygen and glucose deprivation in cortical cell culture: calcium-dependent and calcium-independent mechanisms of neuronal injury. *J Neurosci* **13:** 3510–3524

Gutierrez GJ, Vogtlin A, Castro A, Ferby I, Salvagiotto G, Ronai Z, Lorca T, Nebreda AR (2006) Meiotic regulation of the CDK activator RINGO/Speedy by ubiquitin–proteosome-mediated processing and degradation. *Nat Cell Biol* **8:** 1084–1094

Hansen MB, Nielsen SE, Berg K (1989) Re-examination and further development of a precise and rapid dye method for measuring cell growth/cell killing. *J Immunol Methods* **119:** 203–210

Harada H, Becknell B, Wilm M, Mann M, Huang LJ, Taylor SS, Scott JD, Korsmeyer SJ (1999) Phosphorylation and inactivation of BAD by mitochondria-anchored protein kinase A. *Mol Cell* **3:** 413–422

Hovius R, Lambrechts H, Nicolay K, de Kruijff B (1990) Improved methods to isolate and subfractionate rat liver mitochondria. Lipid composition of the inner and outer membrane. *Biochim Biophys Acta* **1021:** 217–226

Hu G, Zhang S, Vidal M, Baer JL, Xu T, Fearon ER (1997) Mammalian homologs of seven in absentia regulate DCC via the ubiquitin–proteosome pathway. *Genes Dev* **11:** 2701–2714

Huang LJ, Durick K, Weiner JA, Chun J, Taylor SS (1997) Identification of a novel protein kinase A anchoring protein that binds both type I and type II regulatory subunits. *J Biol Chem* **272:** 8057–8064

Hunzicker-Dunn M, Scott JD, Carr DW (1998) Regulation of expression of A-kinase anchoring proteins in rat granulosa cells. *Biol Reprod* **58:** 1496–1502

Irace C, Scorziello A, Maffettone C, Pignataro G, Matrone C, Adornetto A, Santamaria R, Annunziato L, Colonna A (2005) Divergent modulation of iron regulatory proteins and ferritin biosynthesis by hypoxia/reoxygenation in neurones and glial cells. *J Neurochem* **95:** 1321–1331

Li S, Li Y, Carthew RW, Lai ZC (1997) Photoreceptor cell differentiation requires regulated proteolysis of the transcriptional repressor Tramtrack. *Cell* **90:** 469–478

Liu B, Liao M, Mielke JG, Ning K, Chen Y, Li L, El-Hayek YH, Gomez E, Zukin RS, Fehlings MG, Wan Q (2006) Ischemic insults direct glutamate receptor subunit 2-lacking AMPA receptors to synaptic sites. *J Neurosci* **26:** 5309–5319

Livigni A, Scorziello A, Agnese S, Adornetto A, Carlucci A, Garbi A, Castaldo I, Annunziato L, Avvedimento VE, Feliciello A (2006) Mitochondrial AKAP121 links cAMP and src signalling to oxidative metabolism. *Mol Biol Cell* **17:** 263–271

Mullen RJ, Buck CR, Smith AM (1992) NeuN, a neuronal specific nuclear protein in vertebrates. *Development* **116:** 201–211

Nakayama K, Frew IJ, Hagensen M, Skals M, Habelhah H, Bhoumik A, Kadoya T, Erdjument-Bromage H, Tempst P, Frappell PB, Bowtell DD, Ronai Z (2004) Siah2 regulates stability of prolyl-hydroxylases, controls HIF1alpha abundance, and modulates physiological responses to hypoxia. *Cell* **117:** 941–952

Newhall KJ, Criniti AR, Cheah CS, Smith KC, Kafer KE, Burkart AD, McKnight GS (2006) Dynamic anchoring of PKA is essential during oocyte maturation. *Curr Biol* **16:** 321–327

Oliver PL, Bitoun E, Clark J, Jones EL, Davies KE (2004) Mediation of Af4 protein function in the cerebellum by Siah proteins. *Proc Natl Acad Sci USA* **101:** 14901–14906

Pagliarini DJ, Dixon JE (2006) Mitochondrial modulation: reversible phosphorylation takes center stage? *Trends Biochem Sci* **31:** 26–34

Pignataro G, Gala R, Cuomo O, Tortiglione A, Giaccio L, Castaldo P, Sirabella R, Matrone C, Canitano A, Amoroso S, Di Renzo G, Annunziato L (2004) Two sodium/calcium exchanger gene products, NCX1 and NCX3, play a major role in the development of permanent focal cerebral ischemia. *Stroke* **35:** 2566–2570

Scorziello A, Pellegrini C, Secondo A, Sirabella R, Formisano L, Sibaud L, Amoroso S, Canzoniero LM, Annunziato L, Di Renzo GF (2004) Neuronal NOS activation during oxygen and glucose deprivation triggers cerebellar granule cell death in the later reoxygenation phase. *J Neurosci Res* **76:** 812–821

Tang AH, Neufeld TP, Kwan E, Rubin GM (1997) PHYL acts to downregulate TTK88, a transcriptional repressor of neuronal cell fates, by a SINA-dependent mechanism. *Cell* **90:** 459–467

Tasken K, Aandahl EM (2004) Localized effects of cAMP mediated by distinct routes of protein kinase A. *Physiol Rev* **84:** 137–167

Taylor SS, Kim C, Vigil D, Haste NM, Yang J, Wu J, Anand GS (2005) Dynamics of signaling by PKA. *Biochim Biophys Acta* **1754:** 25–37

Wong W, Scott JD (2004) AKAP signalling complexes: focal points in space and time. *Nat Rev Mol Cell Biol* **5:** 959–970